Elimination of Vortex Streets in Bluff-Body Flows

S. Dong,[1,*] G. S. Triantafyllou,[2] and G. E. Karniadakis[3]
[1]*Department of Mathematics, Purdue University, West Lafayette, Indiana 47907, USA*
[2]*National Technical University of Athens, Greece*
[3]*Division of Applied Mathematics, Brown University, Providence, Rhode Island 02912, USA*
(Received 29 August 2007; published 21 May 2008)

We present an effective technique for suppressing the vortex-induced vibrations of bluff bodies by eliminating the von Kármán street formed in their wake. Specifically, we find that small amounts of combined windward suction and leeward blowing around the body modify the wake instability and lead to suppression of the fluctuating lift force. Three-dimensional simulations and stability analysis are employed to quantify our findings for the flow past fixed and flexibly mounted circular cylinders.

DOI: 10.1103/PhysRevLett.100.204501 PACS numbers: 47.32.ck

Vortex shedding from a bluff body is omnipresent in nature and man-made structures. By bluff-body flow we mean flows past blunt objects, such as the wind blowing around a high-rise building or a long bridge, which are opposed to those past a streamlined object such as an aircraft wing. The phenomenon has been studied by several pioneers in fluid dynamics, e.g., Strouhal, Rayleigh, Benard, and von Kármán, and has remained the focus of many modern theoretical and experimental studies [1]. Of interest is the unique Strouhal-Reynolds relationship [2] and also the type of instability that sustains the vortex street, irrespective of any external excitations [3,4]. The asymmetric vortices shed in the bluff-body wake induce large unsteady side forces that, in turn, can lead to large structural vibrations if the body is flexibly mounted, especially in the cross-flow direction [5].

Suppression of the vortex street could reduce such vortex-induced vibrations (VIV) and the wake turbulence, with a direct impact on many engineering applications. To this end, many flow-control techniques have been proposed, e.g., splitter plate, base bleeding, small control cylinder, to name but a few; see [6] for several representative techniques, and [7] for a review of passive control methods. Blowing or suction as a means for cylinder drag reduction or vortex manipulation has also been the subject of several previous studies [8–10]. The ability of blowing or suction to modify the wake has long been recognized [9,11]. For example, by experimentally ejecting or sucking fluid through two rows of small holes on the cylinder surface, Williams *et al.* [9] observed that the produced disturbances significantly modified the pattern and frequencies of vortex shedding and the mean flow. Similarly, in their two-dimensional numerical simulations of a steady suction or blowing applied at the rear stagnation point around the Reynolds number [12] $\mathrm{Re} \approx 47$ (at which the steady flow transitions to an unsteady state with vortex shedding), Delaunay and Kaiksis [10] observed that for $\mathrm{Re} > 47$ slight blowing or sufficiently high suction stabilized the wake while for $\mathrm{Re} < 47$ suction destabilized the wake and blowing had no detectable effect. More recently, Kim and Choi [13] studied a forcing scheme numerically for cylinder drag reduction by blowing or suction of fluid through two slits located on the surface at an angle $\pm 90°$ from the front stagnation line. It was observed that the in-phase forcing from the two slits reduced the drag and could also attenuate or even annihilate the vortex shedding.

There are two fundamental limitations with the flow-control techniques used so far in suppressing vortex-induced vibrations. First, they may be effective only for stationary cylinders (not for flexibly mounted structures). Indeed, it has been shown for some techniques (e.g., wavy cylinders and cylinders with bumps) that even though vortex shedding may be suppressed when the cylinder is fixed, significant oscillations still develop if the cylinder is allowed to freely vibrate [14]. Second, almost all active control schemes proposed require an excessive energy input that makes them impractical at high Reynolds numbers.

The control scheme we propose in the current work addresses both issues. It is very effective in suppressing the vortex street and the vortex-induced vibrations for flexibly mounted structures, and it can readily lead to practical passive control schemes that require no energy input. Specifically, we consider the flow past a long rigid circular cylinder under two situations: the cylinder is (1) fixed (stationary case), and (2) allowed to freely vibrate, but only in the cross-flow direction (VIV case). We investigate the effect of a combined suction and blowing scheme, in which a steady suction is applied on the windward half of the cylinder surface while a steady blowing is applied on the leeward half of the surface. It will be called the WSLB control (WSLB standing for windward suction leeward blowing) hereafter in this Letter. We compare WSLB to two similar schemes: suction-only and blowing-only, with which a steady suction (or blowing) is applied on the entire surface.

We have simulated two Reynolds numbers, $\mathrm{Re} = 500$ and 1000. We solve the three-dimensional incompressible Navier-Stokes equations employing a Fourier expansion along the cylinder axis (or the spanwise direction, in which

 © 2008 The American Physical Society

the flow is assumed to be homogeneous) and a spectral element discretization in the streamwise–cross-flow planes. For the VIV case, the cylinder is elastically mounted and is modeled as a spring-mass oscillation system. The coupled fluid-structure equations are solved in a coordinate system attached to the cylinder axis under which the cylinder becomes stationary. Details of the numerical techniques for the stationary cylinder simulations and for VIV simulations are documented in [15].

The WSLB, suction-only, and blowing-only controls studied here are characterized by a blowing or suction velocity normal to the cylinder surface with a uniform magnitude (hereafter called the control velocity, V_{control}). In the implementation, the Dirichlet boundary condition is applied on the cylinder surface in accordance with the controls; for the case without control, the no-slip condition is imposed. The computational domain extends from $-20D$ at the inlet to $40D$ at the outlet, and from $-20D$ to $20D$ in the cross-flow direction; the spanwise dimension is $3\pi D$. We have performed extensive grid refinement tests with different resolutions, and validation against experimental results; see [16]. Global physical parameters computed from the simulations without control are in good agreement with the experimental data [17]. In the simulations, we have employed a mesh with 1860 quadrilateral elements in the streamwise–cross-flow planes, with the element order and the number of Fourier planes in the spanwise direction 6 and 192, respectively.

The effects of WSLB, suction-only, and blowing-only controls for the stationary case at $\text{Re} = 500$ are compared in Fig. 1(a), in which we plot the root-mean-square (rms) lift coefficient versus V_{control}/U_0. We observe that the fluctuating lift can be significantly reduced, and even completely suppressed at high control velocities. However, the three schemes exhibit quite different characteristics. Suction-only is effective for lift reduction only at high suction velocities. Low suction velocity, on the other hand, appears to have the opposite effect; with $V_{\text{control}}/U_0 = 0.05$ or below, the rms lift coefficient is actually increased. For WSLB the lift coefficient decreases linearly as V_{control} increases and is below a certain value ($0.15U_0$). Beyond this point, the lift coefficient becomes essentially negligible. Both WSLB and suction-only can completely suppress the fluctuating lift at the highest V_{control} considered here ($0.2U_0$). For identical V_{control} WSLB appears more effective than suction-only in terms of lift reduction. With blowing-only, the lift coefficient decreases consistently as V_{control} increases. At $V_{\text{control}}/U_0 = 0.05$ blowing-only appears more effective than the other two schemes; However, as V_{control} increases its rate of lift reduction decreases and it becomes the least effective among the three. At $V_{\text{control}}/U_0 = 0.2$, the fluctuating lift still remains quite significant with this control. Overall, WSLB appears the most effective among the three schemes. At low control velocities it avoids the lift increase with suction-only, while at high control velocities it retains a high rate of reduction, unlike blowing-only. In Fig. 1(b) we demonstrate the effect of Reynolds number with WSLB by plotting the rms lift coefficient versus V_{control} at $\text{Re} = 500$ and 1000 for the stationary case. The lift reduction curve at $\text{Re} = 1000$ shows characteristics similar to that at $\text{Re} = 500$. WSLB control appears equally effective as Reynolds number increases.

To assess the effect of control on free vibrations, we have simulated the flow past a freely oscillating cylinder (in cross-flow direction only) at $\text{Re} = 500$ for two cases: without control and with WSLB control. We have considered only WSLB for the VIV case since results from the stationary case show that it is the most effective among the three. Figure 2(a) shows the rms cylinder displacement (normalized by cylinder diameter) versus V_{control} for two (structural) damping coefficients (0.0046 and 0.046). The cylinder mass ratio (with respect to the fluid) is 5.09. The natural frequency (f_N) of the oscillation is set to be equal to the Strouhal frequency of the flow past a stationary cylinder at the same Reynolds number. By natural frequency we mean the oscillation frequency in the absence of any fluid effects. Evidently, the oscillation amplitude decreases with increasing V_{control}. At high V_{control} values the oscillation is completely suppressed. To further demonstrate the effectiveness of WSLB in VIV reduction, we vary the natural frequency over a range of values. In Fig. 2(b) we plot the rms cylinder displacement versus the reduced velocity, $U_0/(f_N D)$, with and without control, for a fixed

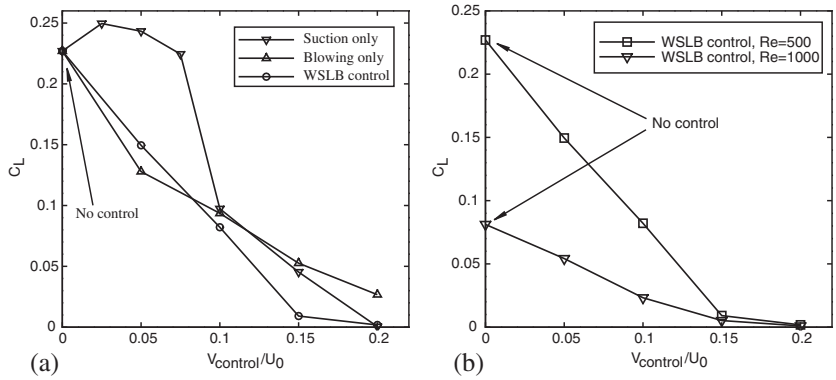

FIG. 1. Vortex street suppression of a stationary cylinder: rms lift coefficient C_L versus normalized control velocity V_{control}/U_0 for different schemes at $\text{Re} = 500$ (a) and for WSLB control at two Reynolds numbers (b).

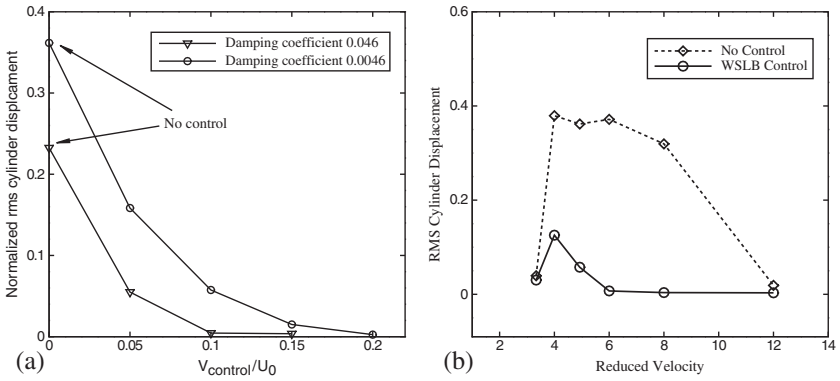

FIG. 2. VIV suppression with WSLB control (freely oscillating cylinder): rms cylinder displacement in cross-flow direction versus the control velocity (a), and versus the reduced velocity (for a fixed control velocity) (b).

$V_{\text{control}}/U_0 = 0.1$ at $\text{Re} = 500$. This is for a damping coefficient 0.0046 and the same mass ratio as before. The control has significantly reduced the oscillation over the entire range of reduced velocity values.

The effects of flow control on wake structures are demonstrated by Fig. 3, in which we plot isosurfaces of the instantaneous intermediate eigenvalue (denoted by λ_2) following the vortex identification method of [18]. These are for the stationary case at $\text{Re} = 500$, without control [Fig. 3(a)] and with WSLB control [Fig. 3(b)]. The wake structures have been significantly modified. Compared to the no-control case, the wake with control is in general depleted of structures. Most notably, the streamwise braids in the near wake have diminished substantially and seem to be clustered at a few spanwise locations. As V_{control} increases, the wake structures become more severely weakened, and at $0.15U_0$ and above the structures vanish from the wake.

To explore the underlying reasons for lift or VIV suppression with flow controls, we have performed a stability analysis [3] of the stationary case. By solving the Orr-Sommerfield equation based on the *mean* streamwise velocity profiles at various downstream (i.e., x) locations, we can determine the coordinates of the "critical point" [3] in the complex frequency ω plane, ω_0. Its imaginary part, ω_I, is related to the growth rate of perturbations, and the sign of ω_I determines the nature of the instability. A positive ω_I indicates an absolute instability, and a negative value indicates a convective instability. Figure 4(a) shows the mapped curves in the ω plane from several lines in the complex wave number plane (ω_R denoting the real part of ω). This is for the downstream location $x/D = 1.0$, without control, at $\text{Re} = 500$. We can clearly observe the critical point (see curve 4).

We have computed ω_0 at several downstream x locations. In Fig. 4(b) we plot ω_I of the critical points versus x for several cases. For the case without control, we observe a region of absolute instability near the cylinder and a region of convective instability further downstream. With WSLB the region of absolute instability shrinks and is displaced downstream; the very near wake also changes from an absolute instability (no control) to a convective instability (see the case $V_{\text{control}}/U_0 = 0.1$). As V_{control} increases, the highest ω_I value in the absolutely unstable region decreases. At $V_{\text{control}}/U_0 = 0.2$ all ω_I have become negative, suggesting a convective instability in the entire wake. As a result, the vortex shedding and the fluctuating lift are completely suppressed. In Fig. 4(c) we plot the loci in the complex ω plane of the critical point $\omega_0(x)$ found from local stability analysis as x is varied. The shapes of the curves suggest the presence of a saddle point in the complex x domain that determines the frequency of the global mode, in agreement with the stability criterion of [4].

In summary, we observe that WSLB is effective to eliminate the vortex street and the VIV in flexibly mounted structures. It is an *active* control scheme requiring external energy input. Regarding how expensive it is, we first note

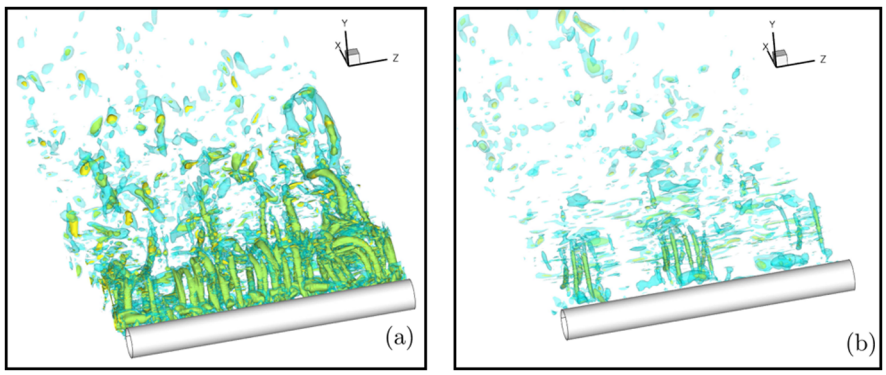

FIG. 3 (color online). Effect of control on wake structures: Isosurfaces of instantaneous $\lambda_2 = -2$ (yellow) and -0.8 (cyan) for flow past a stationary cylinder without control (a) and with the WSLB control ($V_{\text{control}}/U_0 = 0.1$) (b). λ_2 is the intermediate eigenvalue in the method of [18].

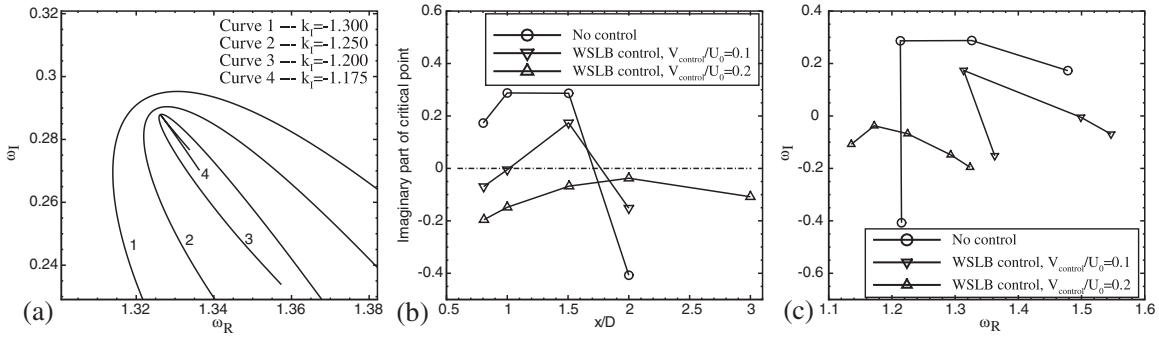

FIG. 4. Stability analysis: (a) Map of lines $k_I =$ constant in the ω plane ($x/D = 1.0$), k being the complex wave number and k_I its imaginary part. The critical point lies at the cusp of curve 4. (b) Imaginary part of the critical point versus streamwise location x. (c) Loci in the complex ω plane of the critical point $\omega_0(x)$ found from local stability analysis as x is varied.

that the required control velocity decreases as the structural damping increases and most surprisingly if periodic on-off control strategies are set along the cylinder axis (results not shown here). With respect to the Reynolds number, we observe that the required normalized control velocities for elimination of vortex street are about the same for Re = 500 and 1000. More importantly, the technique can be easily implemented as a *passive* control scheme by using porous surfaces or by forming communicating channels between the forward and aftward stagnation points of appropriate width. In preliminary simulations, we have tested several such designs, verifying that indeed this is feasible with the required channel width decreasing as Re increases. Results of two recent experiments [19] with designs along this line have supported the findings of this Letter, one with the ''guided porosity'' (flow coming in through holes positioned along the front stagnation line and going out through a row of streamwise-oriented slits located at the top and bottom sides of the cylinder), and the other with a row of holes connecting the front and rear stagnation lines. Regarding the effect on the Strouhal number, we observe in the stationary case that the Strouhal number initially increases slightly with increasing V_{control}, reaching a peak around $V_{\text{control}}/U_0 = 0.1$, and then decreases as V_{control} further increases.

We gratefully acknowledge the support from NSF, ONR, and TeraGrid (computer time), and the useful discussions with Professor M. S. Triantafyllou (MIT).

*Corresponding author.
sdong@math.purdue.edu

[1] T. Leweke, M. Provansal, and L. Boyer, Phys. Rev. Lett. **71**, 3469 (1993); R. Mittal and S. Balachandar, Phys. Rev. Lett. **75**, 1300 (1995); C. Williamson, Annu. Rev. Fluid Mech. **28**, 477 (1996).

[2] F. Ponta and H. Aref, Phys. Rev. Lett. **93**, 084501 (2004); P. Roushan and X. Wu, Phys. Rev. Lett. **94**, 054504 (2005).

[3] G. Triantafyllou *et al.*, Phys. Rev. Lett. **59**, 1914 (1987); P. Huerre and P. Monkewitz, Annu. Rev. Fluid Mech. **22**, 473 (1990).

[4] J. M. Chomaz *et al.*, Stud. Appl. Math. **84**, 119 (1991).

[5] P. Bearman and M. Brankovic, Eur. J. Mech. B, Fluids **23**, 9 (2004); T. Sarpkaya, J. Fluids Struct. **19**, 389 (2004); C. Williamson and R. Govardhan, Annu. Rev. Fluid Mech. **36**, 413 (2004).

[6] A. Roshko, J. Fluid Mech. **10**, 345 (1961); C. Wood, J. R. Aeronaut. Soc. **68**, 477 (1964); P. Strykowski and K. Sreenivasan, J. Fluid Mech. **218**, 71 (1990); C.-J. Wu *et al.*, J. Fluid Mech. **574**, 365 (2007); B. Patnaik and G. Wei, Phys. Rev. Lett. **88**, 054502 (2002).

[7] M. Zdravkovich, J. Wind Eng. Ind. Aerodyn. **7**, 145 (1981).

[8] D. Park *et al.*, Phys. Fluids **6**, 2390 (1994); J.-C. Lin *et al.*, J. Fluids Struct. **9**, 659 (1995); C. Min and H. Choi, J. Fluid Mech. **401**, 123 (1999).

[9] C. Williams *et al.*, J. Fluid Mech. **234**, 71 (1992).

[10] Y. Delaunay and L. Kaiksis, Phys. Fluids **13**, 3285 (2001).

[11] L. Mathelin *et al.*, Int. J. Heat Mass Transf. **44**, 3709 (2001); J. Fransson *et al.*, J. Fluids Struct. **19**, 1031 (2004).

[12] Reynolds number is defined by $\text{Re} = U_0 D/\nu$, where U_0, D, and ν are the free-stream velocity, cylinder diameter, and fluid kinematic viscosity, respectively.

[13] J. Kim and H. Choi, Phys. Fluids **17**, 033103 (2005).

[14] J. Owen and P. Bearman, J. Fluids Struct. **15**, 597 (2001).

[15] S. Dong *et al.*, J. Fluid Mech. **569**, 185 (2006); D. Newman and G. Karniadakis, J. Fluid Mech. **344**, 95 (1997).

[16] S. Dong and G. Karniadakis, J. Fluids Struct. **20**, 519 (2005).

[17] C. Norberg, J. Fluids Struct. **17**, 57 (2003); C. Wieselsberger, Phys. Z. **22**, 321 (1921).

[18] J. Jeong and F. Hussain, J. Fluid Mech. **285**, 69 (1995).

[19] A. Fernandes, N. Coelho, and R. Franchiss, in *Proceedings of the 27th Conference on Offshore Mechanics and Arctic Engineering (OMAE2008), Estoril, Portugal, June 15–20, 2008* (to be published); J. Dahl, Ph.D. thesis, Department of Mechanical Engineering, MIT, Cambridge, MA (2008).